IOP Publishing Classical and Quantum Gravity
Class. Quantum Grav. **37** (2020) 075017 (23pp) https://doi.org/10.1088/1361-6382/ab75ae

Higher dimensional charged compact objects in Finch–Skea geometry

S Dey and B C Paul[1]

Department of Physics, University of North Bengal, Siliguri, Dist. Darjeeling 734 013, West Bengal, India

E-mail: bcpaul@associates.iucaa.in

Received 24 September 2019, revised 7 February 2020
Accepted for publication 12 February 2020
Published 5 March 2020

Abstract

We obtain relativistic solutions of anisotropic charged compact objects in hydrodynamical equilibrium with Finch–Skea geometry in the usual four and in higher dimensions. The relativistic solutions are employed to construct physically viable stellar models. The radial variations of density, pressure and other different physical features inside the stars are studied in the relativistic stellar models. It is noted that a compact star in four-dimensional Finch–Skea geometry describes an isotropic uncharged star always which however predicts existence of an anisotropic star in higher dimensional spacetime. The plausibility of such stars are studied here for a given mass and radius. Considering known compact objects we construct stellar models satisfying all the criteria of a physically realistic star. The results obtained here may be important to understand some of the physical properties of known stars including predictions of equations of states at extreme conditions.

Keywords: higher dimension, charged compact object, gravity

1. Introduction

In the last couple of decades there has been a considerable research activities in higher dimensions to generalize theoretical models and solutions of the standard four-dimensional Einstein theory of gravity. The history of higher dimensions goes back to the independent work reported by Kaluza [1] and Klein [2], to unify gravity with the electromagnetic interaction by introducing the concept of an extra dimension with the usual four dimensions. In astrophysics the concept of the usual four-dimensional space-time embedded in a higher dimensional flat space was put forwarded by Eddington [3]. It has been realized later that the Kaluza–Klein approach does not work well. It was known later that high energy particle physics requires dimensions more than four for their consistent formulations. In recent times it is noticed revival of the

[1] Author to whom any correspondence should be addressed.

concept of the higher dimensions in different aspects of the theoretical research arena. The successes of superstring theories led to a spurt in activities in higher dimensions. Randall and Sundrum [4, 5] proposed a new higher dimensional mechanism for solving the hierarchy problem in addition to the other aspects in brane-world. Consequently, in astrophysics the usual four dimensional results have been generalized, namely, spherically symmetric vacuum solution given by Schwarzschild, Reissner–Nordström black hole [6, 7] metric, Kerr black holes [8], Vaidya solution [9] in the framework of higher dimensions. The mass to radius ratio in higher dimensions for a uniform density star generalized with some predictions by Paul [10]. Emparan and Reall [11] obtained a solution for a black ring in 5 dimensions. Cassisi *et al* [12] explained the effects of higher dimensions on stellar evolution, Yu and Ford [13] reported the observable effects of higher dimensions in the case of light cone fluctuations. At present, higher dimensional theories become an active area of research in understanding the nature at a very high energy scale and in astrophysics. Duorah and Ray [14] found analytic solutions for stellar models for dense stars which found lated that the solutions do not satisfy Einstein's field equations. Later Finch and Skea [15] modified the metric to consider different stellar solutions in the Einstein gravitational action to accommodate some solutions obtained in reference [14] which is known as Finch–Skea [15] metric. The Finch–Skea metric is well behaved and satisfies all the criteria that are required for a physical acceptable stellar models [16]. It describes a strange quark star which obtained considering MIT bag model [17] thereafter considering two-fluids models [18]. Banerjee *et al* [19] showed that a class of interior solutions corresponding to the BTZ black hole [20] as the exterior solution which is admitted in a Finch–Skea geometry in $(3 + 1)$-dimensions.

The gravitational dynamics of a relativistic charged static star may be understood by solving the coupled Einstein–Maxwell equations. The electromagnetic field in a compact object has been an active area of research for many decades. Although Glendenning [21] showed that astrophysical systems are expected to be globally charge neutral at certain evolutionary stages, a charged astrophysical object might originate. Bonnor and Wickramasuriya [22] demonstrated that the electric charge plays a crucial role to obtain equilibrium of a compact object which halts further collapse due to gravitational interaction. The exterior geometry of a static charged spherically symmetric object is uniquely described by the Reissner–Nordström metric. The interior solution of such a system is, however, not unique and a class of physically motivated realistic solutions are reported in the literature which is further reviewed by Ivanov [23]. Stettner [24] showed that a homogeneous fluid sphere with a considerable amount of surface charge density is more stable than that of an uncharged sphere. A class of relativistic charged star solutions in higher dimensions using Vidya–Tikekar metric is reported in reference [25]. Recently, realistic solutions of Einstein–Maxwell equations describing various aspects of astrophysical objects, have been developed and analyzed.

The origin of anisotropy in a compact star in the presence of strong electric field has been studied by Usov [26]. It is also pointed out that the matter inside a compact object may be anisotropic at a nuclear density $\sim 10^{15}$ g cm^{-3}, where nuclear interactions can be treated relativistically, which was originally considered by Ruderman [27]. Charged anisotropic models with a linear equation of state was considered by Thirukkanesh and Maharaj [28]. Further, Takisa and Maharaj [29] generated regular solutions of anisotropic spherically symmetric object with charge distributions considering a linear equation of state.

The anisotropy is an important issue which arises due to the fact that in the high-density regime in compact stars the radial pressure (p_r) and the transverse pressure (p_t) are unequal which has been proposed by Canuto [30]. The shear of the fluid may be considered as another reason for origin of anisotropy in a self gravitating body [31]. Another view is that the slow

rotation of fluids, a mixture of perfect and null fluids may be considered as the origin of an effective anisotropic fluid in a compact star.

Hansraj and Maharaj [32] showed that the Finch–Skea geometry describes a realistic charged compact object in four−dimensions. It was noted that the relativistic solution for the Einstein–Maxwell equations corresponds to Bessel functions or modified Bessel functions of different situations. Maharaj *et al* [33] also adopted a technique to obtain a class of solutions of such relativistic equations which describes an anisotropic charged compact star with Finch–Skea geometry. Consequently, a class of exact solutions can be obtained from the field equations in terms of elementary functions to obtain different stellar models. Relativistic solutions of the Einstein–Maxwell equations corresponding to a spherically symmetric charged sphere using Finch–Skea metric in four-dimensions is studied and the electromagnetic field effect on the M–R relationship of compact stars also analyzed in reference [34].

The isotropic fluid distribution in a Finch–Skea metric extended to higher dimensions has been studied by Chilambwe and Hansraj [35]. Dadhich *et al* [36] obtained the pure Lovelock analogue with Finch–Skea geometry and established similarity in solutions for the critical odd and even $d = 2N + 1, 2N + 2$ dimensions. Recently, Paul and Dey [37] obtained new relativistic solutions with Finch–Skea geometry in the usual four and in higher dimensions. It is noted that an uncharged compact star in four-dimensions with Finch–Skea geometry always accommodates an isotropic compact object which however admits an anisotropic star if the space-time dimension is more than the usual four-dimensions. The motivation of the present paper is to obtain relativistic models of compact stars in higher dimensional Finch–Skea geometry with anisotropic fluid distribution and/or charge star. As the matter inside the compact object is not yet known at the extreme conditions, the equation of state will be determined in addition to the radial variations of different physical features making use of the technique considered in the literature [38]. In the absence of any reliable information about the equation of state (EoS) at extreme densities assumption of the metric potentials predicts the EoS. We consider here Finch–Skea geometry to construct both charged and uncharged stellar models accommodating all the necessary criterion for a physically viable stellar model that are mentioned by Delgaty and Lake [16]. The objective of the paper is to obtain relativistic solutions in a higher dimensional Finch–Skea metric to construct relativistic stellar models in higher dimensions. The relativistic solutions will be used to study compact objects with electric field or anisotropy or presence of both anisotropy and electromagnetic field in the higher dimensional Finch–Skea geometry. As the size of a compact star is not yet known accurately we study stellar models with a definite mass to estimate radius of a compact object for different parameters for accommodating neutron or quark stars.

The paper is organized as follows: in section 2, we present field equations governing the spherically symmetric static charged compact objects corresponding to the Einstein–Maxwell equations in D-dimensions. By assuming a particular form of the electric field the anisotropy of the model can be calculated in the Finch–Skea background spacetime. The expressions of these parameters are determined and different special cases permitted here are discussed. In section 3, the exterior region of the charged fluid distribution is described by the Reisner–Nordström metric and the junctions conditions joining the interior and the exterior regions are matched at the boundary of the stars. In section 4, we study physical features of compact objects e.g. radial variation of electric field, energy-density, pressures, anisotropy and surface charge density in the usual four and in dimensions more than the usual four dimensions. We analyze the stability conditions of an anisotropic charged star, different energy conditions and mass–radius relation also. In section 5, we tabulate the range of different metric parameters for realistic solutions of stellar models and their variations with dimensions and in section 6, equation of states are predicted. Finally, in section 7 we discuss the results obtained.

2. Einstein–Maxwell field equation in higher dimensions and solution

The Einstein's field equation is given by,

$$R_{ab} - \frac{1}{2} g_{ab} R = k^2 T_{ab}, \tag{1}$$

where, $k^2 = \frac{8\pi G_D}{c^2}$, D is the total number of dimensions, $G_D = GV_{D-4}$ is the gravitational constant in D dimension and V_{D-4} is the volume of the extra space, R_{ab} is Ricci tensor and T_{ab} is the energy-momentum tensor. We consider the metric of a higher dimensional spherically symmetric, static spacetime which is given by,

$$\mathrm{d}s^2 = -\mathrm{e}^{2\nu(r)}\mathrm{d}t^2 + \mathrm{e}^{2\lambda(r)}\mathrm{d}r^2 + r^2\mathrm{d}\Omega_n^2, \tag{2}$$

where, $\nu(r)$ and $\lambda(r)$ are the two unknown metric functions, $n = D - 2$ and $\mathrm{d}\Omega_n^2 = \mathrm{d}\theta_1^2 + \sin^2\theta_1\mathrm{d}\theta_2^2 + \sin^2\theta_2(\mathrm{d}\theta_3^2 + \ldots. + \sin^2\theta_{n-1}\mathrm{d}\theta_n^2)$ represents the metric on the n-sphere in polar coordinates. The energy momentum tensor for a charged star in higher dimensions is given by,

$$T_{ab} = \mathrm{diag}\,(-(\rho + E^2), p_\mathrm{r} - E^2, p_\mathrm{t} + E^2, \ldots., p_\mathrm{t} + E^2), \tag{3}$$

where, ρ is the energy density, p is pressure and E represents the electric field.

The components of Einstein field equation equation (1) using equations (2) and (3) are given by

$$\frac{n(n-1)\left(1 - \mathrm{e}^{-2\lambda}\right)}{2r^2} + \frac{n\lambda'\mathrm{e}^{-2\lambda}}{r} = k^2(\rho + E^2), \tag{4}$$

$$\frac{n\nu'\mathrm{e}^{-2\lambda}}{r} - \frac{n(n-1)\left(1 - \mathrm{e}^{-2\lambda}\right)}{2r^2} = k^2(p_\mathrm{r} - E^2), \tag{5}$$

$$\mathrm{e}^{-2\lambda}\left(\nu'' + \nu'^2 - \nu'\lambda' - \frac{(n-1)(\lambda' - \nu')}{r}\right) - \frac{(n-1)(n-2)\left(1 - \mathrm{e}^{-2\lambda}\right)}{2r^2} = k^2(p_\mathrm{t} + E^2), \tag{6}$$

where overheads prime denotes the derivative w.r.t. the radial coordinate r. Using equations (5) and (6), the electric field can be written as

$$E^2 = \frac{1}{2\mathrm{e}^{2\lambda}}\left(\nu'' + \nu'^2 - \nu'\lambda' - \frac{(n-1)\lambda'}{r} - \frac{\nu'}{r} - \frac{(n-1)\left(1 - \mathrm{e}^{2\lambda}\right)}{r^2}\right) \tag{7}$$

Now consider the interior spacetime given by Finch–Skea metric as,

$$\mathrm{e}^{\lambda(r)} = \sqrt{1 + C\,r^2}, \tag{8}$$

$$\mathrm{e}^{\nu(r)} = \left(B - A\sqrt{1 + C\,r}\right)\cos\sqrt{1 + C\,r^2} + \left(A + B\sqrt{1 + C\,r^2}\right)\sin\sqrt{1 + C\,r^2} \tag{9}$$

where A, B and C are unknown constants, prescribing the specific geometries for the three-space of the interior spacetime of a compact object it is possible to investigate various physical features of dense stars. For different values of the metric parameters we construct stellar models for known mass of stars making use of the boundary conditions.

The total electric charge in higher dimensions is given by

$$q(r) = 4\pi \int_0^r \sigma r^n \mathrm{e}^{\lambda} \mathrm{d}r = r^n\, E(r), \tag{10}$$

where σ denotes the proper charge density. The electric field E is determined using $\lambda(r)$ and $\nu(r)$ from equations (8) and (9) in equations (5) and (6) respectively, which is given by,

$$E = \sqrt{\frac{1}{2}\left(\frac{C^2(n-2)r^2}{(1+C\,r^2)^2} - \Delta\right)} \tag{11}$$

where $\Delta = p_{\mathrm{t}} - p_{\mathrm{r}}$ represents the anisotropy in pressure.

We note the following special cases:

Case (i): in four-dimensions (i.e., $n = 2$), an isotropic uncharged star [23] is obtained.

Case (ii): in higher dimensions (i.e. $n > 2$), it corresponds to an anisotropic uncharged star $E^2 = 0$ with an anisotropy given by

$$\Delta = p_{\mathrm{t}} - p_{\mathrm{r}} = \frac{C^2(n-2)r^2}{(1+C\,r^2)^2}, \tag{12}$$

which depends on the space-time dimensions and metric parameter inside the star.

Case (iii): in higher dimensions (i.e. $n > 2$), an isotropic charged star is permitted. In this case the electric field is determined as follows

$$E^2 = \frac{C^2(n-2)r^2}{2(1+C\,r^2)^2}. \tag{13}$$

It may be pointed out here that similar features is obtained in $D = 4$ dimensions with modified Finch–Skea metric [33, 34]. We also note a new result that an isotropic charged star with electric field in higher dimensional original Finch–Skea metric can be obtained in higher dimensions.

Case (iv): in higher dimensions (i.e. $n > 2$), a new class of stellar models can be obtained here with both non zero electric field with anisotropic fluid distribution. In this case the anisotropy and the electric field intensity are determined by considering a fractional distribution between them as $\alpha = \frac{\Delta}{2E^2}$. The sum total of electric field intensity and anisotropy is a constant. Increase in anisotropy leads to a decrease in electric field and vice versa. Now, the electric field intensity can be expressed as,

$$E^2 = \frac{C^2(n-2)r^2}{2\,(1+\alpha)\,(1+C\,r^2)^2}, \tag{14}$$

and then the anisotropic parameter becomes

$$\Delta = 2\alpha\, E^2 = \frac{C^2(n-2)r^2\alpha}{(1+\alpha)\,(1+C\,r^2)^2}, \tag{15}$$

both the electric field and the anisotropic parameter are zero at the center of the compact object. Both the Electric field and anisotropic parameter are non-zero away from the center and these are regular functions inside the compact objects. One gets only electric field given by equation (13) when $\alpha = 0$.

Case (v): we note here an interesting case in lower dimensions where the role of radial pressure and transverse pressure changes when $\alpha < -1$. It leads to $E^2 > 0$ with $\Delta < 0$, demanding radial pressure being greater than the tangential pressure i.e., $p_{\mathrm{r}} > p_{\mathrm{t}}$. It may be pointed out that

Δ is regular at the center (beginning as $p_r = p_t$ at the center) and a wide range of anisotropy can be obtained for $D < 4$ with $\alpha > -1$. This case permits stellar models only in the framework $(2+1)$-dimensional Finch–Skea metric. However $-1 < \alpha < 0$ leads to charged star with $p_r > p_t$ which implies $\Delta < 0$.

Therefore, physical features of a star namely, the radial variations of the energy density (ρ), the radial pressure (p_r) of a relativistic charged star can be obtained from equations (4) and (5) using the metric potentials $\lambda(r)$ and $\nu(r)$ given by Finch–Skea metric in higher dimensions which are

$$\rho = \frac{C(2Cr^2 + n^2K'^2(1+\alpha) + nX_0)}{2k^2K'^4(1+\alpha)}, \tag{16}$$

$$p_r = \frac{C}{k^2}\left[\frac{n\,X'}{K'^2\,X_1} + \frac{n(1-n)}{2K'^2} + \frac{(n-2)(K'^2-1)}{2(1+\alpha)K'^4}\right], \tag{17}$$

where we denote $K' = \sqrt{1+Cr^2}$, $X_1 = (B - AK')\cos K' + (A + BK')\sin K'$ and $X' = B\cos K' + A\sin K'$, $X_0 = (1 + \alpha - Cr^2(2+\alpha))$.

The tangential pressure is $p_t = p_r + \Delta$. The surface charged density is obtained from equation (10), which can be expressed as,

$$\sigma = \frac{C\sqrt{(n-2)}(1+n-C\,r^2+C\,nr^2)}{4\sqrt{2}\pi(1+Cr^2)^{5/2}\sqrt{1+\alpha}}, \tag{18}$$

Using equation (14), the central energy density of a charged star is determined and found that it is independent of r i.e. the charge density is a constant at the center for a given dimension $(n = D-2)$ which is given by,

$$\rho_0 = \frac{C[(D-2)+(D-2)^2]}{2k^2}, \tag{19}$$

The central density is determined by the metric parameter C and space-time dimensions D. For $C > 0$ the central density is always positive definite and increases with increase in number of extra dimensions for $D > 2$. The electric field E^2 can be determined from equation (12), it admits anisotropic charged star for $D > 4$ with $0 < \alpha < 1$. For $n = 2$ the energy density and pressure corresponds to uncharged, isotropic star, which admits only in four dimensions. It is observed from equations (14)–(16) that ρ, p_r and σ satisfies simple functional forms which are well behaved, bounded, finite and regular at the center. The stellar models namely, an x-ray pulsar Her X-1 characterised by mass $M = 0.88M_\odot$, where $M =$ the solar mass, size of the star $b = 7.7$ km [25,39] and a massive neutron star PSR J0348 + 0432 [40] which my contain hyperons [41] are considered to construct stellar models in section 5.

3. Physical criterion of charged stellar model

To obtain viable stellar models we impose the following necessary conditions:

- At the boundary of a higher dimensional charged star (i.e. $r = b$), the interior solution should be matched with the exterior Reissner–Nördstrom metric in higher dimensions, given by

$$ds^2 = -\left[1 - \frac{K}{r^{n-1}} + \frac{q^2}{r^{2(n-1)}}\right]dt^2 + \left[1 - \frac{K}{r^{n-1}} + \frac{q^2}{r^{2(n-1)}}\right]^{-1}dr^2 + r^2 d\Omega_n^2, \tag{20}$$

i.e., at the boundary of the star ($r = b$), we match $e^{2\nu(r=b)} = e^{-2\lambda(r=b)} = \left[1 - \frac{K}{b^{n-1}} + \frac{q^2}{b^{2(n-1)}}\right]$ where q denotes the total charge of the compact star as measured by an observer at infinity and the corresponding mass in the absence of EM field. The mass of a star is given by $M = \frac{nA_nK}{16\pi G_D}$ and $G_D = GV_{D-4}$ with $V_n = \frac{\pi^{\frac{n}{2}} r^n}{\Gamma(\frac{n}{2}+1)}$.

- The radial pressure (p_r) drops from its maximum value (at center) to zero at the boundary, i.e., at $r = b$, $p_{r=b} = 0$.
- Inside the charged sphere, the density and the pressures should be positive.
- To maintain the causality condition the speed of sound must satisfy the inequality $v^2 = \frac{dp}{d\rho} \leqslant 1$, which leads to stability [42].
- In general, for a charged fluid sphere in equilibrium with nonzero pressure, $M^2 > q^2$ (CooperStock and De La Cruz [43])
- The gradient of the pressure and energy-density should be negative inside the stellar configuration, i.e., $\frac{dp_r}{dr} < 0$ and $\frac{d\rho}{dr} < 0$.
- The metric potentials $\nu(r)$, $\lambda(r)$ given by equation (2) and the electric field intensity E should be positive and non singular inside the star.
- At the center of the star, $\Delta(0) = 0$ which implies zero radial and tangential pressure, $p_r(0) = p_t(0)$.
- The charged anisotropic fluid sphere must satisfy the following three energy conditions, viz., (a) null energy condition (NEC), (b) weak energy condition (WEC) and (c) strong energy condition (SEC).
- The adiabatic index $\Gamma = \frac{\rho+p}{p}\frac{dp}{d\rho} > \frac{4}{3}$ required to satisfy for ensuring stability of the stellar configuration (Heintzmann and Hilebrandt) [44].

4. Physical analysis of compact objects

In this section we examine the physical properties of compact objects:

4.1. Variation of electric field and charged density with dimensions

The radial variation of the electric field E^2 is plotted in figure 1. It is found that electric field intensity increases away from the center but the variation decreases as it approaches the boundary. For a given value of the parameter α the electric field intensity also increases with the increase in dimensions of the spacetime (D). For $D = 4$ it reduces to an uncharged star. Thus existence of extra dimension leads to charged stars. Thus, the Finch–Skea metric admits charged star in higher dimensions which however remains uncharged in four-dimensions. This is a new result. The radial variation of proper charge density (σ) with various dimensions for a given α is plotted in figure 2. It is found that the charge density is maximum at the center which however decreases toward the boundary. The charge density also increases with increase in dimensions for a given mass and radius of the star.

4.2. Energy-density and radial pressure in higher dimensions

In this section, the radial variation of ρ and p_r are plotted for $D = 4, 5, 6, 7$ in figures 3 and 4 respectively. The density of the charged star is maximum at the center which decreases radially outward. The radial pressure decreases away from the center which vanishes at the boundary.

The plot of transverse pressure with radius in figure 5, follows the same behavior in different framework of dimensions. It is evident from figures 4 and 5 that both p_r and p_t are same at the center of the star, which, however, branches away toward the boundary of the star. It is evident

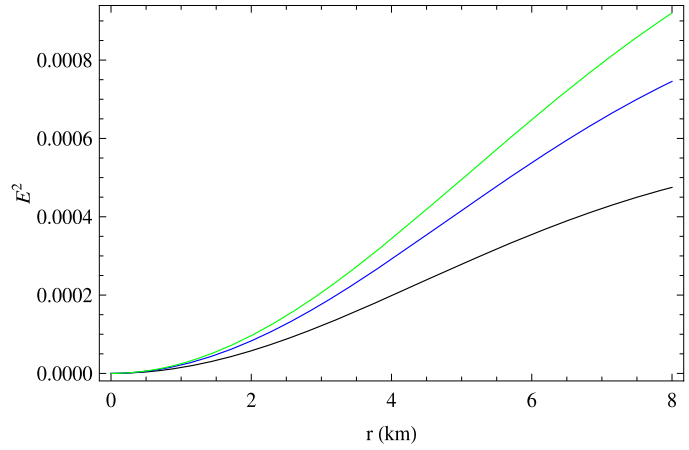

Figure 1. Radial variation of E^2 at the stellar interior of the pulsar Her X-1 for $D = 5$ (black), $D = 6$ (blue) and $D = 7$ (green) considering $\alpha = 0.5$.

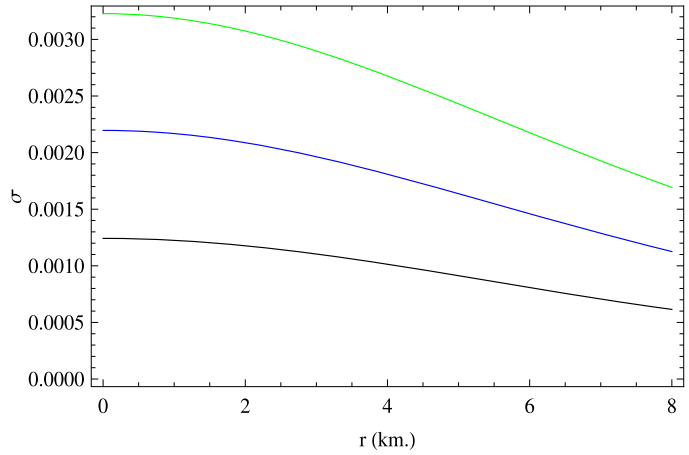

Figure 2. Radial variation of σ at the stellar interior of the pulsar Her X-1 for $D = 5$ (black), $D = 6$ (blue) and $D = 7$ (green) considering $\alpha = 0.5$.

that both the energy-density (ρ) and the radial pressure (p_r) are higher for a charged compact object (for $D > 4$) compared to the uncharged star (for $D = 4$). The variation of the energy-density and radial pressure gradients with dimensions are plotted in figures 6 and 7, it is clear that they are negative inside the star.

4.3. Anisotropy in pressure

In figure 8 radial variation of Δ is plotted for $D = 5, 6, 7$. For a given α as the space-time dimension increases it incorporates more anisotropy inside the star. In figure 9 the variation of Δ and electric field intensity (E^2) are plotted for an increase in α. It is evident that as α increases anisotropy increases and electric field intensity decreases. Thus α plays an important role in deciding the anisotropic pressure distribution inside a compact object for a given charge

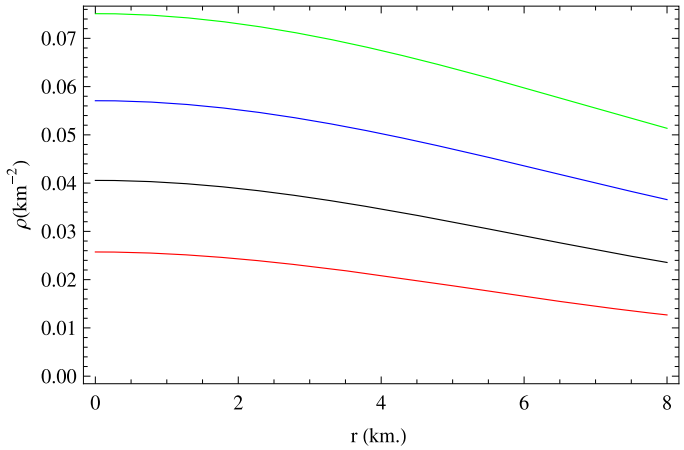

Figure 3. Radial variation of energy-density (ρ) in Her X-1 for $D = 4$ (red), $D = 5$ (black), $D = 6$ (blue) and $D = 7$ (green) in the unit of G_D (considering $\alpha = 0.5$).

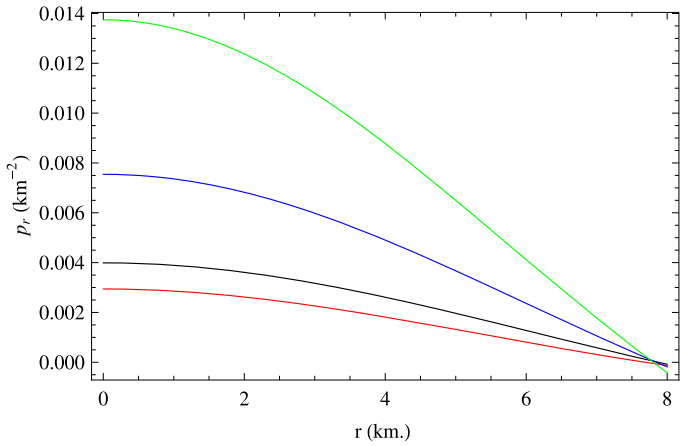

Figure 4. Radial variation of p_r in Her X-1 for $D = 4$ (red), $D = 5$ (black), $D = 6$ (blue) and $D = 7$ (green) in units of G_D (considering $\alpha = 0.5$).

configuration. It represents the sharing between E^2 and Δ for a given star. In figure 9, we plot both E^2 and Δ inside Her X-1 (with size $b = 7.7$ km) for α which varies from 0 to 1. It is also evident that $\Delta > 0$, for $p_t > p_r$ which in turn implies that the anisotropic stress is directed outwards, hence there exists a Coulomb repulsive force which dominates over the gravitational attraction, consequently it may lead to formation of super-massive stars in more than four-dimensions. Thus, we note that the anisotropic charged stars in higher dimensional Finch–Skea geometry are possible which however are not permitted in four-dimensions.

4.4. Stability study

4.4.1. Herrera's cracking concept. The stability of a stellar model is studied by plotting square of the radial speed of sound (v_r^2) and square of the transverse speed of sound (v_t^2) with r in

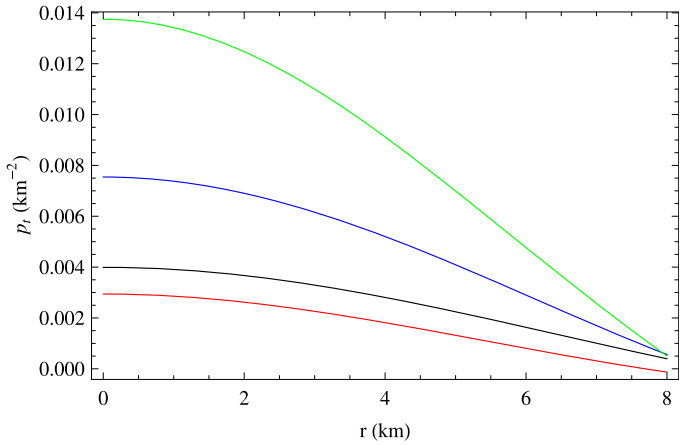

Figure 5. Radial variation of p_t in Her X-1 for $D = 4$ (red), $D = 5$ (black), $D = 6$ (blue) and $D = 7$ (green) in units of G_D (considering $\alpha = 0.5$).

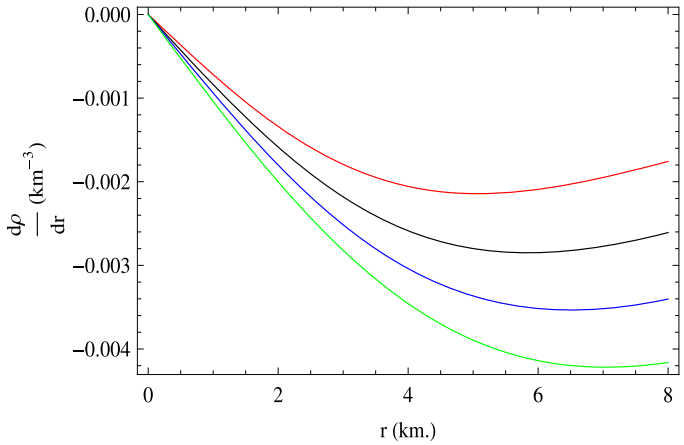

Figure 6. Radial variation of $\frac{d\rho}{dr}$ in Her X-1 for $D = 4$ (red), $D = 5$ (black), $D = 6$ (blue) and $D = 7$ (green) (considering $\alpha = 0.5$).

figures 10 and 11 respectively. It is evident that one obtains stellar models in higher dimensions, where v_r^2 and v_t^2 always less than 1. Consequently, a stable configuration of an anisotropic charged compact object can be accommodated [42].

4.4.2. Adiabatic index. In a compact star there is no heat transfer from or to the compact system (or any isolated gravitating object), consequently it may be considered as an adiabatic system which obeys the equation of state namely, $pV^{\Gamma} = \text{constant}$, where $\Gamma =$ adiabatic index. The adiabatic index for the radial pressure is

$$\Gamma_r = \frac{\rho + p_r}{p_r}\frac{dp_r}{dr} = \frac{\rho + p_r}{p_r}v_r^2, \tag{21}$$

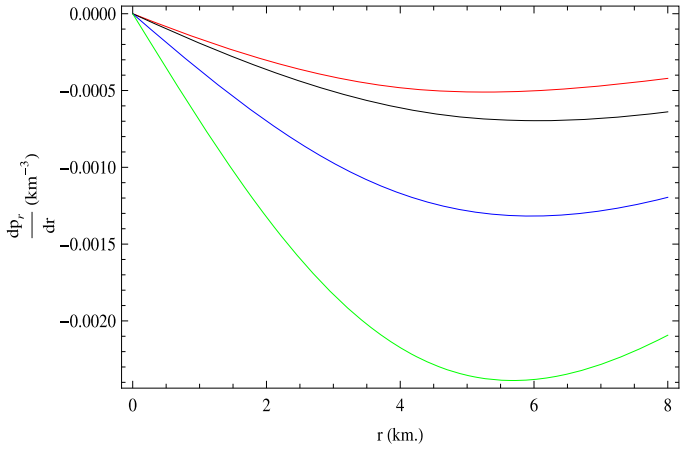

Figure 7. Radial variation of $\frac{dp_r}{dr}$ in Her X-1 for $D = 4$ (red), $D = 5$ (black), $D = 6$ (blue) and $D = 7$ (green) (considering $\alpha = 0.5$).

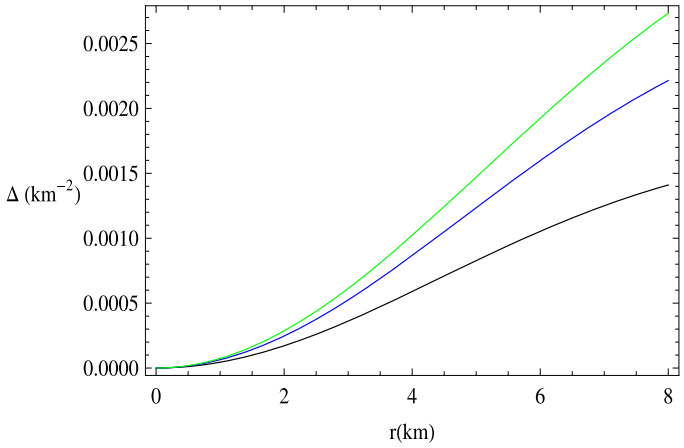

Figure 8. Radial variation of Δ at the stellar interior of the pulsar Her X-1 for $D = 5$ (black), $D = 6$ (blue) and $D = 7$ (green) (considering $\alpha = 0.5$).

and the adiabatic index for the tangential pressure is

$$\Gamma_t = \frac{\rho + p_t}{p_t}\frac{dp_t}{dr} = \frac{\rho + p_t}{p_t}v_t^2, \tag{22}$$

It is to be noted that the conventional condition for the stability with adiabatic contraction of a Newtonian isotropic sphere is $p \sim \rho^{\Gamma}$, provided that $\Gamma \geq \frac{4}{3}$ [44]. Therefore for a relativistic stable isotropic sphere it is also considered $\Gamma > \frac{4}{3}$ due to the presence of regenerative effect of pressure and even it is also applicable in the case of a radial pulsating neutron star. However, for an anisotropic relativistic sphere the situation becomes more complicated and the stability

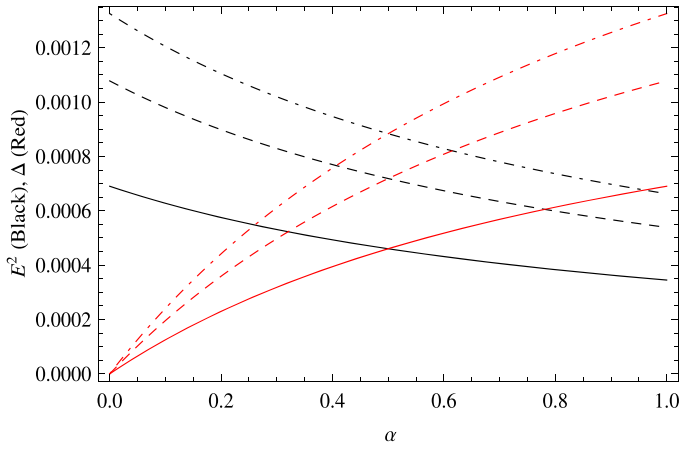

Figure 9. Variation of E^2(black) and Δ(red) inside Her X-1 with α for $D = 5$ (solid line), $D = 6$ (dashed) and $D = 7$ (dot dashed) (considering $b = 7.7$ km).

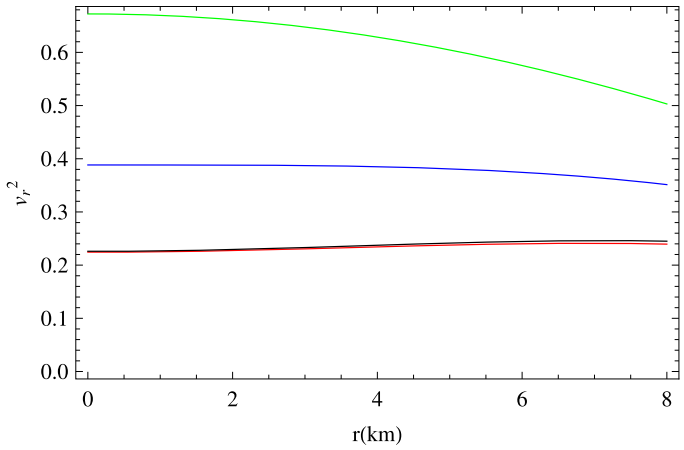

Figure 10. Radial variation of v_r^2 at the stellar interior of the pulsar Her X-1 for $D = 4$(red), $D = 5$ (black), $D = 6$ (blue) and $D = 7$ (green) (considering $\alpha = 0.5$).

condition for an anisotropic fluid is given by [45,46]:

$$\Gamma_r, \Gamma_t > \frac{4}{3} + \frac{4}{3}\left[\frac{p_{t0} - p_{r0}}{|p'_{r0}|r} + \frac{2\pi\rho_0 p_{r0} r}{|p'_{r0}|}\right], \tag{23}$$

where p_{r0}, p_{t0} and ρ_0 are the initial radial, tangential, and energy density respectively. The first and last terms inside the square bracket represent the anisotropic and relativistic corrections respectively and both the quantities are positive which increases the range of Γ. It is evident from figures 12 and 13 that both the radial and tangential adiabatic index satisfies the inequality $\Gamma_r > \Gamma_t$ throughout the star and hence the stellar model is stable. The tangential pressure in the higher dimensional compact object always dominates and increases with a higher rate than that of the radial pressure. On the other hand the adiabatic index satisfies an inverse relation with pressure, therefore, $\Gamma_r > \Gamma_t$. At the surface of the compact object, Γ_r

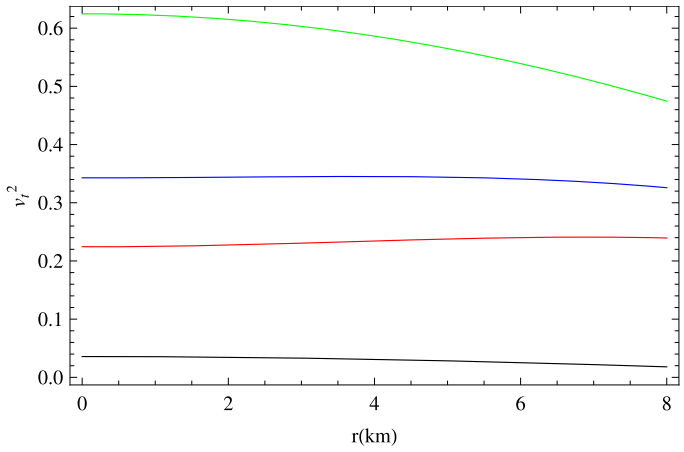

Figure 11. Radial variation of $v_{\rm t}^2$ at the stellar interior of the pulsar Her X-1 for $D = 4$(red), $D = 5$ (black), $D = 6$ (blue) and $D = 7$ (green) (considering $\alpha = 0.5$).

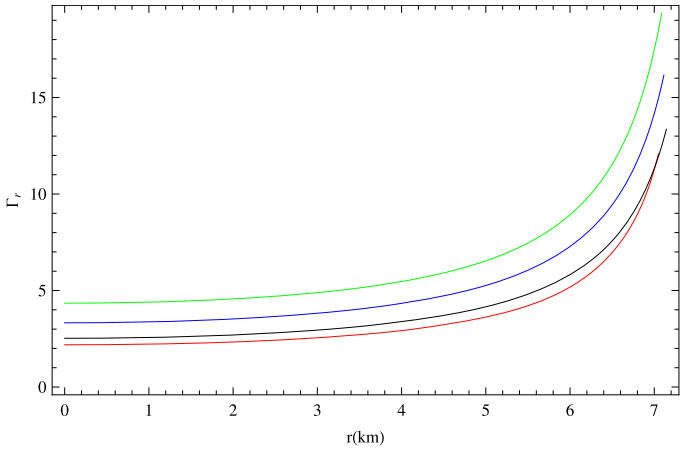

Figure 12. Behavior of $\Gamma_{\rm r}$ at the stellar interior of the pulsar Her X-1 for $D = 4$ (red), $D = 5$ (black), $D = 6$ (blue) and $D = 7$ (green) (considering $\alpha = 0.5$).

increases more rapidly than $\Gamma_{\rm t}$. The above result is because of the fact that the radial pressure decreases more rapidly near the surface than that of the tangential pressure. Thus stable anisotropic compact charged star is possible to accommodate in Finch–Skea metric in higher dimensions.

4.5. Energy conditions

The charged anisotropic fluid sphere satisfies the following three energy conditions, *viz.*, (i) null energy condition (NEC), (ii) weak energy condition (WEC) and (iii) strong energy condition (SEC). We note the following inequalities:

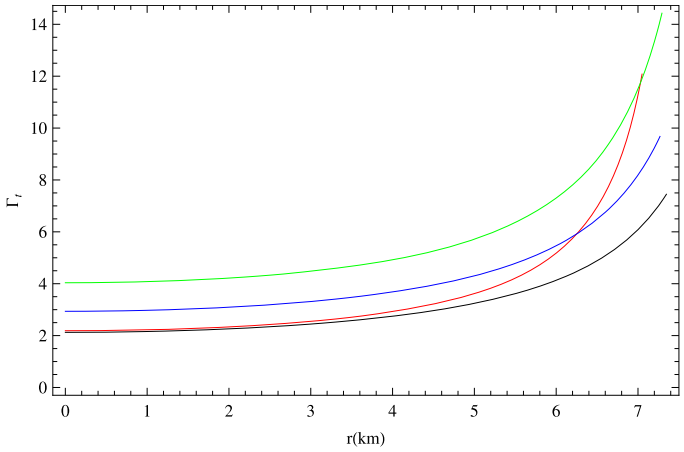

Figure 13. Behavior of Γ_r at the stellar interior of the pulsar Her X-1 for $D = 4$ (red), $D = 5$ (black), $D = 6$ (blue) and $D = 7$ (green) (considering $\alpha = 0.5$).

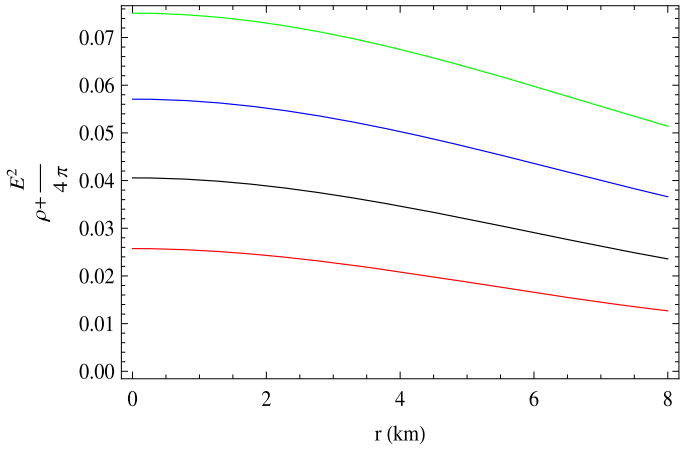

Figure 14. Behavior of NEC inside Her X-1 for $D = 4$ (red), $D = 5$ (black), $D = 6$ (blue) and $D = 7$ (green) (considering $\alpha = 0.5$).

$$\text{NEC}: \rho + \frac{E^2}{8\pi} \geq 0, \tag{24}$$

$$\text{WEC1}: \rho + p_r \geq 0; \qquad \text{WEC2}: \rho + p_t + \frac{E^2}{4\pi} \geq 0, \tag{25}$$

$$\text{SEC}: \rho + p_r + 2p_t + \frac{E^2}{4\pi} \geq 0, \tag{26}$$

The plots in figures 14–17, in support of the energy conditions corresponding to equations (24)–(26), for a specific stellar configuration.

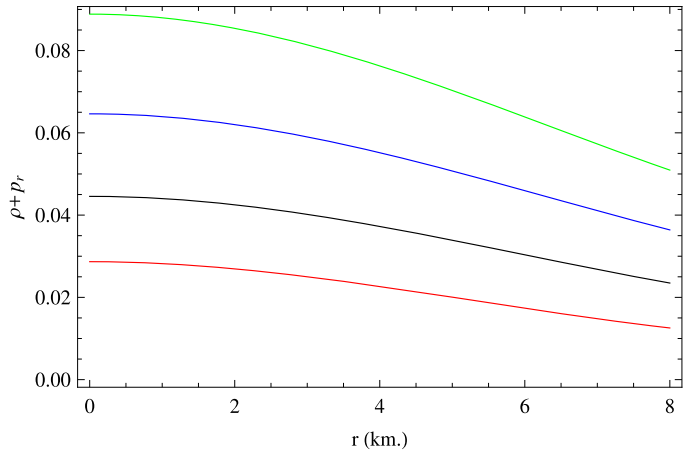

Figure 15. Behavior of WEC1 inside Her X-1 for $D = 4$(red), $D = 5$ (black), $D = 6$ (blue) and $D = 7$ (green) (considering $\alpha = 0.5$).

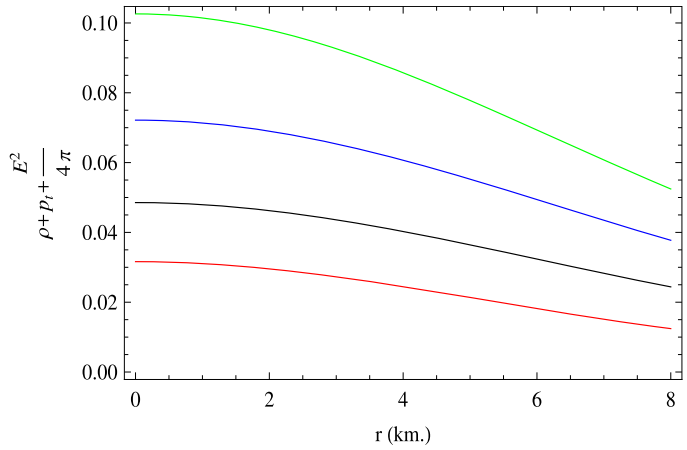

Figure 16. Behavior of WEC2 inside Her X-1 for $D = 4$(red), $D = 5$ (black), $D = 6$ (blue) and $D = 7$ (green) (considering $\alpha = 0.5$).

4.6. Mass–radius relationship

The total mass of a charged star contained within radius r in D-dimension is given by,

$$m(r) = A_n \int_0^r r'^{D-2} \left[\rho(r') + \frac{E^2(r')}{8\pi}\right] \mathrm{d}r', \tag{27}$$

where, $A_n = \frac{2\pi^{\frac{n+1}{2}}}{\Gamma\left(\frac{n+1}{2}\right)}$ and $\rho(r')$ represents the energy density at $r' = r$. We consider Her X-1 with observed mass equal to $0.88M_\odot$ [25,47]. Now plotting the observed mass in the mass–radius curve in figure 18, it is found that one can predict the variation of the size of a compact object. For uncharged case (i.e. $D = 4$) to charged cases (in higher dimensions, $D > 4$) the radius may vary. In a higher dimensional case the size of a star may be lower

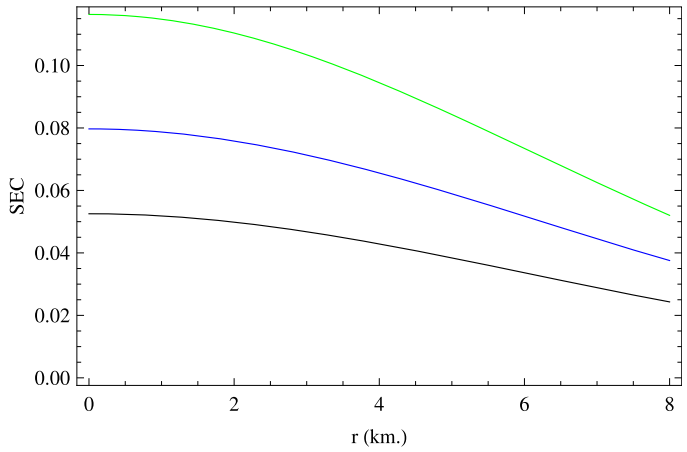

Figure 17. Behavior of SEC inside Her X-1 for $D = 4$(red), $D = 5$ (black), $D = 6$ (blue) and $D = 7$ (green) (considering $\alpha = 0.5$).

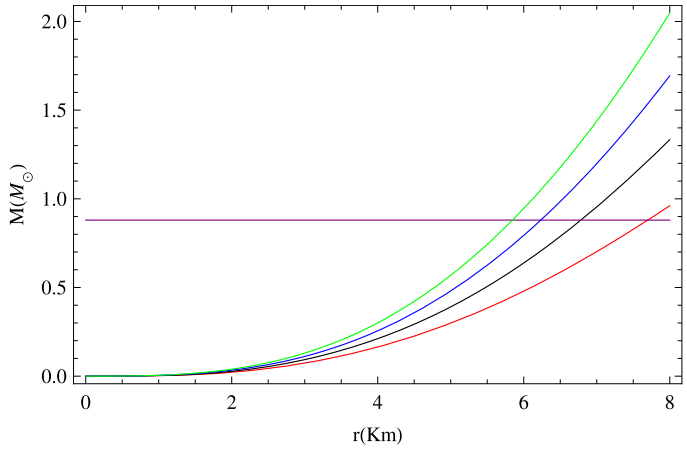

Figure 18. Radial variation of mass inside Her X-1 for $D = 4$(red), $D = 5$ (black), $D = 6$ (blue) and $D = 7$ (green) (considering $\alpha = 0.5$).

than 7.7 km, which accommodates a charged anisotropic star. From figure 18 it is found that for a given mass the radius decreases with increase in dimensions, thus mass to radius relation is also known as the compactness factor increases in higher dimensions. It is also noted that for a given radius, the total mass increases with an increase in charge density because the electric energy density adds on to the mass energy density and its variation is more effective near the boundary of the star. As it is not yet measured the radius of a star accurately, many aspects of a compact object may be understood once the mass and radius are determined accurately.

Table 1. Different values of parameters A, B, C for Her X-1 considering $\alpha = 0.5$.

D	A	B	C
4	0.2721	0.4489	0.008 578
5	0.7572	0.3272	0.006 760
6	1.3028	0.1900	0.005 707
7	1.8792	0.0464	0.005 007
8	2.4742	0.1004	0.004 502
9	2.5522	0.4757	0.010 895
10	3.6985	0.3993	0.003 812

Table 2. Different values of parameters A, B, C for PSR J0348 + 0432 considering $\alpha = 0.5$.

D	A	B	C
4	0.3153	0.2625	0.009 664
5	0.677 49	0.1748	0.006 967
6	1.134 17	0.0524	0.005 608
7	1.6406	0.0835	0.004 771
8	2.1775	0.2262	0.004 198
9	1.6891	0.8054	0.013 922
10	3.3067	0.5217	0.003 454

Table 3. Different values of parameters A, B, C in $D = 4$ and $D = 5$ for pulsar Her X-1 considering $\alpha = 0.5$.

$D = 4$				$D = 5$			
r	A	B	C	r	A	B	C
14	0.221 95	0.565 91	0.001 161	14	0.782 03	0.433 46	0.000 952
13	0.227 06	0.555 58	0.001 476	13	0.777 44	0.424 73	0.001 207
12	0.232 93	0.543 31	0.001 917	12	0.772 07	0.414 39	0.001 561
11	0.239 70	0.528 65	0.002 552	11	0.765 71	0.401 98	0.002 070
10	0.2477	0.510 67	0.003 506	10	0.758 02	0.386 89	0.002 825
9	0.257 12	0.488 21	0.005 0045	9	0.748 52	0.368 08	0.004 002
8	0.268 34	0.459 28	0.007 5060	8	0.736 47	0.343 98	0.005 938
7	0.281 69	0.420 58	0.012 03	7	0.720 57	0.311 97	0.009 372
6	0.297 20	0.366 02	0.021 18	6	0.6984	0.267 33	0.016 115
5	0.3130	0.282 88	0.043 19	5	0.6646	0.200 57	0.031 494
4	0.3147	0.139 69	0.115 56	4	0.6037	0.089 31	0.076 546

5. Variations of metric parameters with dimensions in charged star

The parameters A, B and C in Finch–Skea metric given by equations (8) and (9) are determined in terms of space-time dimensions (D). The parameters are determined in four-dimensions for a given mass and radius of a star. It is noted that the model can be extended for higher dimensions upto $D = 7$ for the parameters with allowed values that are tabulated in tables 1 and 2 for Her X-1 and PSR J0348 + 0432 respectively. From table 1, it is evident that Her X-1

Table 4. Different values of parameters A, B, C in $D = 4$ and $D = 5$ for PSR J0348 + 0432 considering $\alpha = 0.5$.

$D = 4$				$D = 5$			
r	A	B	C	r	A	B	C
14	0.295 72	0.374 292	0.003 748	14	0.701 76	0.274 03	0.002 863
13	0.302 28	0.344 305	0.004 962	13	0.689 61	0.249 70	0.003 737
12	0.3093	0.307 86	0.006 783	12	0.674 82	0.220 40	0.005 015
11	0.315 31	0.262 55	0.009 664	11	0.656 26	0.184 37	0.006 9684
10	0.318 26	0.204 71	0.014 56	10	0.631 97	0.139	0.010 128
9	0.313 15	0.127 77	0.023 841	9	0.598 23	0.080 06	0.015 65

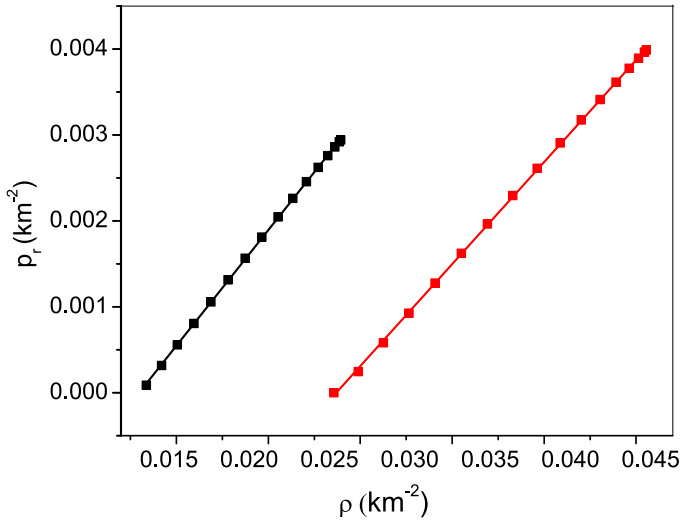

Figure 19. Curve fitting of p_r^* with ρ^* in Her X-1 for $D = 4$(black), $D = 5$ (red).

can be considered in $D = 4$ which can be embedded in $D = 5$ to $D = 7$. It is found that Her X-1 does not permit space-time dimension more than 7 as unphysical results cropped up ($v^2 > 1$ and $M^2 < Q^2$) here. Similarly, from table 2 it is evident that PSR J0348 + 0432 permitted in $D = 4$ can be embedded to $D = 5$ and $D = 6$ dimensions, as for $D \geq 7$ PSR JO348 + 0432 it gives rise unphysical result ($v^2 > 1$).

The metric parameters A, B and C for both $D = 4$ and $D = 5$ dimensions for a range of values of radius i.e. from $R = 4$ km to $R = 14$ km for Her X-1 using Finch–Skea metric are presented in table 3. For PSR J0348 + 0432, the metric parameters A, B and C for $D = 4$ and $D = 5$ dimensions are presented in table 4. In this case we consider a range size for PSR J0348 + 0432 taken from $R = 9$ km to $R = 14$ km. For PSR J0348 + 0432 it is noted that $R \leq 9$ km is not permitted in both $D = 4$ and $D = 5$ dimensions. Thus it is noted that stellar models namely, HER X1 and PSR J0348 + 0432 can be accommodated with radius lying between 4 km to 14 km for different parameters, this is the reported observed range for radius for neutron star.

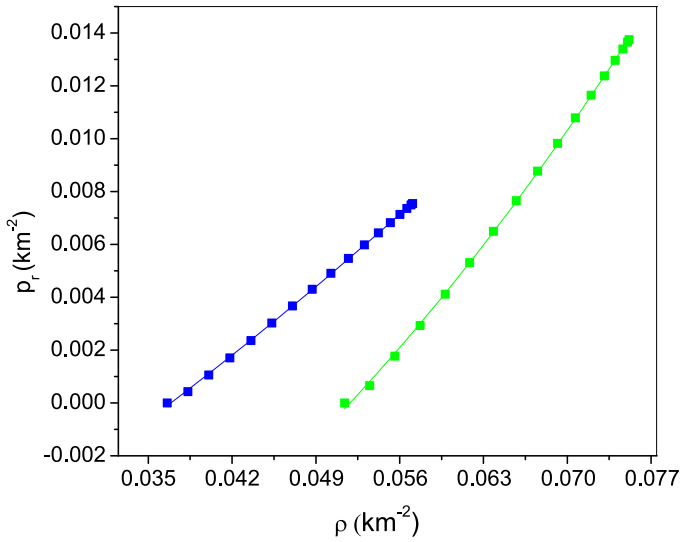

Figure 20. Curve fitting of $p_{\rm r}^{*}$ with ρ^{*} in Her X-1 for $D = 6$(blue), $D = 7$ (green).

6. Equation of state (EoS)

The parametric plot of radial pressure and density is employed here to determine the equation of state (EoS). It is highly non-linear, we analyze and fit the curves to express pressure as a function of density. The effective energy density and pressure of the system are given by:

$$p_{\rm r}^{*} = p_{\rm r} - \frac{E^2}{8\pi} \quad \text{and} \quad \rho^{*} = \rho + \frac{E^2}{8\pi}, \tag{28}$$

for obtaining EoS. We plot $p_{\rm r}^{*}$ against ρ^{*} making use of the equation (28) which is shown in figures 19 and 20 for $D = 4$ and $D = 5$ dimensions respectively. Finally, we find the best fitted relations for Her X-1. It is found that EoS for Her X-1 is linear for $D = 4$ and $D = 5$, but non-linearity develops in figure 20 as the number of dimension increases say for, $D = 6$ and $D = 7$.

7. Discussion

We obtain a class of relativistic solutions for static compact charged stars in a higher dimensional Finch–Skea geometry. For realistic stellar models the interior solutions of Einstein–Maxwell equations for a charged compact object is matched with that of the Reissner–Nördstrom metric at the boundary. A higher dimensional geometry described by Finch–Skea metric is considered to explore the effect of dimensions in the compact objects. We consider two known stars, namely Her X-1 and PSR J0348 + 0432. Her X-1 is characterized by its mass, $M = 0.88M_{\odot}$, where $M_{\odot}$ represents the solar mass with a size of the star $b = 7.7$ km [25,47] (values within the experimental ranges of mass and radius of Her X-1). We note the following:

(a) The radial variation of ρ, $p_{\rm r}$ and $p_{\rm t}$ for $D = 4$ to $D = 7$ dimensions are plotted in figures 3–5 respectively. The energy density and the radial pressure are found well behaved

inside the compact object. Both the energy-density (ρ) and the radial pressure (p_r) begins from higher values which then decreases away from the center. In the case of higher dimension ($n > 2$) as the number of space-time dimensions increases the density and pressure also increases. The central density is found to increases with the increase in the number of extra dimensions in the theory. The plot of variations of the energy-density and radial pressure gradients with dimensions are shown in figures 6 and 7, which are negative inside.

(b) It is found that the relativistic solutions in higher dimensions admits charged stars in higher dimensions. The plot of radial variation of E^2 in figure 1 show that it increases away from the center to the periphery. As the number of extra dimensions is increased it leads to a compact star with more electric field at the surface. In figure 2, the radial variation of proper charged density (σ) is plotted for a given dimension. It is evident that the charge density is more at the center which also increases with the increase in number of extra dimension and away from the center it decreases.

(c) In four-dimensions one gets that $\Delta = 0$ leads to an isotropic star. However, as the spacetime dimensions (n) is increased the stellar model here allows an anisotropic compact star which is shown in figure 8. It is noted that as one moves away from the center there is a branching away of the radial and tangential pressures and once again it is found that it increases with the increase in number of extra dimensions. Here the anisotropic parameter Δ is always positive which means $p_t > p_r$, which implies that the anisotropic stress is directed outwards, thus there exists a coulomb repulsive force dominating over the gravitational attraction in a charged star. It allows the formation of super-massive stars in a higher dimensions. In figure 9, the electric field intensity E^2 and Δ inside Her X-1 are plotted for different values of the fractional distribution α. In Her X-1 (considering $b = 7.7$ km), varying α from 0 to 1 it is evident that while E^2 decreases Δ increases and *vice-versa* which are plotted for $D = 5$ to $D = 7$ dimensions. For a given lower values of α it is electric field that dominates over the anisotropy. Thus there exist an interplay between E^2 and Δ.

(d) The solutions obtained here reduces to an isotropic star with charge when $\alpha = 0$, in higher dimensions which follow from equations (12) and (13). A number of new and interesting cases are obtained here which are enumerated in section 2 as observed from case (i) to case (v).

(e) The variation of the radial and transverse speeds of sound are plotted in figures 10 and 11 respectively. The stellar models found here are stable as v_r and $v_t \ll 1$.

(f) The adiabatic indices Γ_r and Γ_t are plotted in figures 12 and 13 respectively which are greater than $\frac{4}{3}$. It is clear that both the radial and tangential adiabatic index follow the inequality $\Gamma_r > \Gamma_t$ throughout the star and hence the stability of the models are ensured once again.

(g) In figures 14–17, the radial variation of the energy conditions, viz., (a) null energy condition (NEC), (b) weak energy condition (WEC) and (c) strong energy condition (SEC) are plotted for different space-time dimensions. It is found that the stellar models obtained here are realistic for a set of model parameters.

(h) The mass radius plot in figure 18 for different dimensions shows that the size of a compact star for a given mass may be different. As the number of dimensions increases the star may accommodate more mass and lesser radius than the usual four dimensions. It is also evident that for a given radius, the total mass increases with an increase in charge density because the electric energy density adds on to the mass energy density.

Table 5. Predicted EoS for Her X-1 in different dimensions taking $\alpha = 0.5$.

Dimensions(D)	Equation of states (EoS)
4	$p_r = 0.234\rho - 0.003$
5	$p_r = 0.237\rho - 0.005$
6	$p_r = 1.4131\rho^2 + 0.241\,93\rho - 0.0108$
7	$p_r = 4.5303\rho^2 + 0.016\,83\rho - 0.0130$

(i) The metric parameters A, B and C of Finch–Skea metric are determined for consistent stellar models for $D = 4$ to $D = 10$ dimensions. In table 1 for we presented the values, and it is seen that as D increases A also increases with various values of B and C. In table 2 we present the values of A, B and C for PSR J0348 + 0432. It is evident that Her X-1 can be accommodated in $D = 4$ upto $D = 7$ dimensions as $D \geq 8$, leads to unphysical result. Similarly, from table 2 it is evident that for PSR J0348 + 0432 can be accommodated for $D \geq 7$. Thus we note that spacetime dimensions here plays an important role in describing a given known star for higher dimensional Finch–Skea geometry.

(j) The effective energy density (ρ^*) and the effective radial pressure (p_r^*) are determined for a given set of values of the model parameters and a best fitted curve can be drawn as the EoS does not correspond to any known functional form. In the case of Her X-1, in $D = 4$ and $D = 5$, the EoS of the star are found linear, which becomes non-linear in $D = 6$ and $D = 7$ as presented in table 5. A deviation from linearity is visible due to the incorporation of charges in higher dimensions. The variation of p_r^* with ρ^* are shown in figures 19 and 20 in different dimensions.

(k) The metric parameters A, B and C for both $D = 4$ and $D = 5$ dimensions for Her X-1 are determined using Finch–Skea metric. We consider a range of size i.e., from $R = 4$km to $R = 14$km shown in table 3. For PSR J0348 + 0432 we also determined the metric parameters A, B and C for $D = 4$ and $D = 5$ dimensions in table 4 and here we have seen that the acceptable range for PSR J0348 + 0432 is from $R = 9$km to $R = 14$km using Finch–Skea metric. It is found that PSR J0348 + 0432 can be accommodated with lowest size $R = 9$km both $D = 4$ and $D = 5$ dimensions. The other compact stars will be taken up elsewhere. We can estimate the size of the compact star knowing its mass which can be accommodated over a wide range of values of the radius depending on the model parameters. As the actual size of a star is not known accurately in future the model may give an acceptable estimation with its physical features.

Thus in a higher dimensional Finch–Skea geometry we obtained relativistic solutions which can be employed to construct stellar models of different kinds. The parameters of the model plays an important role to estimate the radii of compact objects. We consider two such stars and determine the radii of those stars satisfying the observed limits for neutron star by a variation of the model parameters.

Acknowledgment

S D thankful to UGC-CSIR, India for awarding financial support. We thank the anonymous referees for their useful feedback. B C P would like to thank DST-SERB (Grant No. EMR/2016/005734) Govt. of India for a project. B C P and S D would like to thank IUCAA,

Pune for supporting a visit to carry out research work and Inter-University Center for Astronomy Research and Development (ICARD), North Bengal University. We are thankful to unanimous referee for suggestion and criticism to present the paper in its current form.

ORCID iDs

B C Paul https://orcid.org/0000-0001-5675-5857

References

[1] Kaluza T 1921 *Sitz. Preuss. Acad. Wiss.* **33** 966
[2] Klein O A 1926 *Z. Phys.* **37** 895
[3] Eddington A S 1924 *The Mathematical Theory of Relativity* (Cambridge: Cambridge University Press)
[4] Randall L and Sundrum R 1999 *Phys. Rev. Lett.* **83** 3370
[5] Randall L and Sundrum R 1999 *Phys. Rev. Lett.* **83** 4690
[6] Myers R C and Perry M J 1986 *Ann. Phys.* **172** 314
[7] Shen Y and Tan Z 1989 *Phys. Lett. A* **142** 341
[8] Mazur P O 1989 *J. Math. Phys.* **28** 406
[9] Iyer B and Vishveshwara 1989 *Pramana J. Phys.* **32** 749
[10] Paul B C 2001 *Class. Quantum Grav.* **18** 2637
[11] Emparan R and Reall H S 2002 *Phys. Rev. Lett.* **88** 101101
[12] Cassisi S *et al* 2000 *Phys. Lett. B* **481** 323
[13] Yu H and Ford L H 1999 Lightcone fluctuations in quantum gravity and extra dimensions arXiv:gr-qc/9907037
[14] Duorah H L and Ray R 1987 *Class. Quantum Grav.* **4** 1691
[15] Finch M R and Skea J E F 1989 *Class. Quantum Grav.* **6** 467
[16] Delgaty M S R and Lake K 1998 *Comput. Phys. Commun.* **115** 395
[17] Kalam M, Usmani A A, Rahamani F, Hossein S M, Karar I and Sharma R 2013 *Int. J. Theor. Phys.* **52** 3319
[18] Kalam M, Rahamani F, Ray S, Hossein S M, Karar I and Naska J 2013 *Eur. Phys. J. C* **73** 2049
[19] Banerjee A, Rahamani F, Jotania K, Sharma R and Karar I 2013 *Gen. Relativ. Gravit.* **45** 717
[20] Banados M, Teitelboim C and Zanelli J 1992 *Phys. Rev. Lett.* **69** 1849
[21] Glendenning N K 2000 *Compact Stars: Nuclear Physics, Particle Physics, and General Relativity* (Berlin: Springer)
[22] Bonnor W B and Wickramasuriya S B P 1975 *Mon. Not. R. Astron. Soc.* **170** 643
[23] Ivanov B V 2002 *Phys. Rev. D* **65** 104011
[24] Stettner R 1973 *Ann. Phys.* **80** 212
[25] Chattopadhyay P, Deb R and Paul B C 2014 *Int. J. Theor. Phys.* **53** 1666
[26] Usov V V 2004 *Phys. Rev. D* **70** 067301
[27] Ruderman R 1972 *Astron. Astrophys.* **10** 427
[28] Thirukkanesh S and Maharaj S D 2008 *Class. Quantum Grav.* **25** 235001
[29] Takisa P M and Maharaj S D 2013 arXiv:1310.0433
[30] Canuto V 1974 *Annu. Rev. Astron. Astrophys.* **12** 167
[31] di Prisco A, Herrera L, Le Denmat G, MacCallum M A H and Santos N O 1980 *Phys. Rev. D* **76** 064017
[32] Hansraj S and Maharaj S D 2006 *Int. J. Mod. Phys. D* **15** 1311
[33] Maharaj S D, Kileba Matondo D and Takisa P M 2017 *Int. J. Mod. Phys. D* **26** 1750014
[34] Ratanpal B S, Pandya D M, Sharma R and Das S 2017 *Astrophys. Space Sci.* **362** 82
[35] Chilambwe B and Hansraj S 2015 *Eur. Phys. J. Plus* **130** 19
[36] Dadhich N, Hansraj S and Chilambwea B 2017 *Int. J. Mod. Phys. D* **26** 1750056
[37] Paul B C and Dey S 2018 *Astrophys. Space Sci.* **363** 220
[38] Paul B C 2004 *Int. J. Mod. Phys. D* **13** 229
[39] Lattimer J 2010 http://stellarcollapse.org/nsmasses/2010

[40] Antoniadis *et al* 2013 *Science* **340** 448
[41] Zao X A 2017 *Acta Phys. Pol. B* **48** 171
[42] Herrera L 1992 *Phys. Lett. A* **165** 206
[43] CooperStock F I and De La Cruz V 1978 *Gen. Relativ. Gravit.* **9** 835
[44] Heintzmann H and Hillebrandt W 1975 *Astron. Astrophys.* **38** 51
[45] Chan R, Herrera L and Santos N O 1992 *Class. Quantum Grav.* **9** 133
[46] Chan R, Herrera L and Santos N O 1993 *Mon. Not. R. Astron. Soc.* **265** 533
[47] Sharma R and Mukherjee S 2001 *Mod. Phys. Lett.* **16** 1049